GA–A22885

A TANGENTIALLY VIEWING VUV TV SYSTEM FOR THE DIII–D DIVERTOR

by
D.G. NILSON, G. BREWIS, R. ELLIS, M.E. FENSTERMACHER,
N. JALUFKA, and R.T. SNIDER

JULY 1998

DISCLAIMER

GA–A22885

A TANGENTIALLY VIEWING VUV TV SYSTEM FOR THE DIII–D DIVERTOR

by
D.G. NILSON,† G. BREWIS,‡ R. ELLIS,† M.E. FENSTERMACHER,†
N. JALUFKA,◊ and R.T. SNIDER

This is a preprint of a paper presented at the 12th Topical Conference on High-Temperature Plasma Diagnostics, June 7–11, 1998, Princeton, New Jersey and to be published in *Review of Scientific Instruments.*

†Lawrence Livermore National Laboratory
‡Allied Optical
◊Center for Fusion Research and Training, Hampton University

Work supported by
the U.S. Department of Energy
under Contracts DE-AC03-89ER51114, W-7405-ENG-48,
and Grant 97ER54451

GA PROJECT 3466
JULY 1998

ABSTRACT

A video camera system capable of imaging VUV emission in the 120–160 nm wavelength range, from the entire divertor region in the DIII–D tokamak, was designed. The new system has a tangential view of the divertor similar to an existing tangential camera system [M.E. Fenstermacher *et.al.*, Rev. Sci. Instrum., 68, 974 (1997)] which has produced two dimensional maps of visible line emission (400–800 nm) from deuterium and carbon in the divertor region. However, the overwhelming fraction of the power radiated by these elements is emitted by resonance transitions in the ultraviolet, namely the C IV line at 155.0 nm and Ly-α line at 121.6 nm. To image the ultraviolet light with an angular view including the inner wall and outer bias ring in DIII–D, a 6-element optical system (*f*/8.9) was designed using a combination of reflective and refractive optics. This system will provide a spatial resolution of 1.2 cm in the object plane. An intermediate UV image formed in a secondary vacuum is converted to the visible by means of a phosphor plate and detected with a conventional CID camera (30 ms framing rate). A single MgF_2 lens serves as the vacuum interface between the primary and secondary vacuums; a second lens must be inserted in the secondary vacuum to correct the focus at 155 nm. Using the same tomographic inversion method employed for the visible TV, we will reconstruct the poloidal distribution of the UV divertor light. The grain size of the phosphor plate and the optical system aberrations limit the best focus spot size to 60 μm at the CID plane. The optical system is designed to withstand 350°C vessel bakeout, 2 T magnetic fields, and disruption-induced accelerations of the vessel.

I. INTRODUCTION

A detailed understanding of the power balance in present tokamak divertors is required for validation of divertor simulation codes which can then be used to predict the performance of divertor designs in future high power tokamaks. A key piece of the power balance physics is to determine the radiating constituents which contribute to the total radiated power from the divertor. To validate 2-dimensional scrape-off-layer (SOL) and divertor models, the 2D spatial profile of radiation from each of the radiating species is required. Tangentially viewing video camera systems are valuable diagnostics for obtaining 2D emission data in tokamak divertors.[1]

Radiation emitted from the divertor plasma in the DIII–D tokamak is primarily from carbon and deuterium. The carbon source is from graphite tiles which cover the entire vessel wall; deuterium radiation comes from the main plasma working gas. Visible imagery has shown[2] that carbon tends to radiate closer to the X–point in the divertor; deuterium radiates closer to the target plates. This conclusion was obtained from reconstructions of emission profiles in a poloidal plane from 3D data taken by a tangentially viewing camera with visible wavelength filters.[1] However, line radiation from the vacuum ultraviolet (VUV) wavelength range (90–160 nm) contributes the largest fraction of the radiated power in the DIII–D divertor. The two lines which dominate the radiation are the CIV emission at 155 nm and the Ly-α radiation at 121.6 nm. A VUV SPRED spectrograph[3,4] which provides a vertical line integrated measurement in the divertor was used to determine the contributions of these lines. Other lines which contribute are CIII at 97.7 and 117.5 nm and Ly-β at 102.5 nm. For DIII–D radiative divertor scenarios, CIV emission at 155 nm is key to the formation of the detached plasma with reduced heat flux to the target plates. The Ly-α radiation may play a key role in the deuterium recombination physics which leads to the reduction in ion flux to the target plates in this mode.

This paper describes the development of a tangentially viewing diagnostic to image the CIV (155 nm) and Ly-α (121.6 nm) radiation in the entire divertor region of DIII–D. The paper is organized as follows. Section II describes the hardware that was developed to relay the VUV image out of a radial vacuum vessel port on DIII–D. The light then passes through a wavelength filter and onto a VUV-to-visible phosphor which is imaged by a CID video camera. Section III gives sample images from first data obtained with the system. Conclusions are presented in Section IV.

II. HARDWARE

The goal of the instrument that was developed for and installed on DIII–D was to bring an image of VUV emission from the divertor region out of the tokamak for documentation by a visible video camera. The DIII–D tokamak environment presented a number of difficult constraints that affected the optical design of this instrument. First, since there is no available tangentially (toroidally) viewing port on DIII–D, the optics system had to relay an image of the divertor emission with a tangential line-of-sight through a radial reentrant tube (see Fig. 1). The image plane needed to be at a location sufficiently outside the vessel so that the camera could operate without interference from stray magnetic fields from the tokamak coils. Second, the system had to be able to withstand the 350°C vessel baking temperature. This precluded duplicating the re-entrant vacuum window and lens coupled fiberoptic system that was used on the existing visible tangential TV system because commercially available MgF_2 windows cannot withstand this temperature. Instead, a combination of high temperature reflective elements and lower temperature refractive elements were used to relay the image. The two MgF_2 refractive elements are limited to low angles of incidence (and therefore low optical power) due to the birefringence of this material. Lithium Flouride is the only other optical material that transmits well at these wavelengths, but it was not considered as a lens material due to poor mechanical properties. Other optical design concerns included: a) achieving sufficient throughput with a large number of elements, b) providing a 2 m depth of field for image inversion analysis, and c) designing a system with a field of view that would cover the entire divertor region.

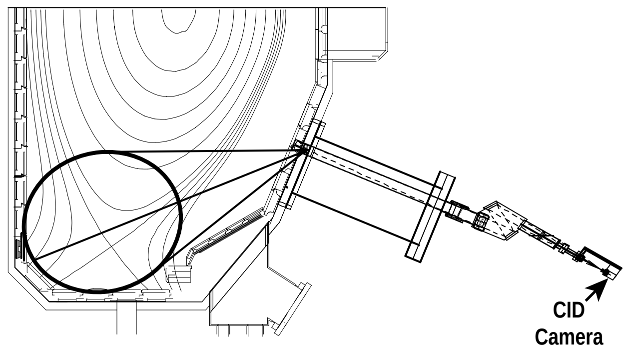

Fig. 1. The new VUVTTV produces a 3D image of the DIII–D divertor region by relaying a toroidal view through a radial tube, onto a CID camera located outside the vessel.

The optical system that was chosen is a catadioptric design with a field of view of approximately 26°. The basic layout shown in Fig. 2 is that of a three mirror WALRUS configuration (Wide Angle Large Reflective Unobscured System). This relayed system has, in addition, a fold mirror which serves as the aperture stop (4.5 mm diameter) at the location of the entrance pupil and a powered vacuum window (lens) made of MgF_2. The two mirrors closest to the image plane have an inverse Cassegrain form. The overall system has a working f-number of *f*/8.9 and a magnification of 0.023. The image is captured on a P1 phosphor (7.5 mg/cm^2) coated on a fused silica substrate and is fixed along the optical axis for both wavelegths of interest. However, the lateral image position and its magnification do change with wavelength. The fixed image plane is made possible by using an additional MgF_2 lens for viewing at 155 nm and a separate BK7 lens for alignment at 632.8 nm. Calculations show that less than 5% of the incident flux at 155 nm becomes stray light due to the birefringence of MgF_2. The oxygen partial pressure in the secondary chamber containing the final two mirrors and focus lens must be reduced to avoid the strong absorption of VUV emission in the range of interest (especially for the 155 nm radiation). This can be done either by active pumping during operations or by backfilling with nitrogen to atmospheric pressure. A 25 mm *f*/1.4 lens

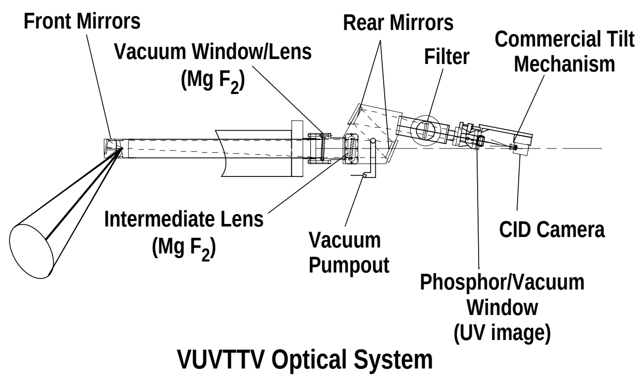

Fig. 2. The optical system is a catadioptric design with a field of view of approximately 26°, a magnification of 0.023, and a working f-number of f/8.9. The basic layout is that of a three mirror WALRUS configuration (Wide Angle Large Reflective Unobscured System).

relays the phosphor image onto a CIDTEC CID camera and the data is then stored on magnetic VCR tape for future digitization and analysis.

Wavelength selection is provided by a narrowband transmission filter placed between the final aluminum mirror and the phosphor. The FWHM for the 155nm and 121.6 nm filters are 22 nm and 11 nm respectively. The two in-vessel mirrors at the front of the optics system are coated with tungsten which has a predicted reflectivity of 50% at 155 nm and 25% at 121.6 nm. These mirrors should reach 280°C during vessel bakout which is within the allowable operating temperature of the tungsten coatings. The final two mirrors are coated with aluminum and a MgF_2 overcoat, and should have reflectivities exceding 65% at the two wavelengths. Since these mirrors are located a meter from the vessel wall, they do not exceed 100°C during vessel bakeout, and are therefore under the allowable temperature limit for the aluminum coatings.

All component reflection and transmission values have been tabulated and the resulting overall predicted transmission is calculated for the two wavelengths of interest (see Table I). These estimates indicate that the system

Table I
System Component Efficiencies

Element	Efficiency at 1550Å	Efficiency at 1216Å
Mirror 1	>50% Reflectivity	>25% Reflectivity
Mirror 2	>50% Reflectivity	>25% Reflectivity
MgF_2 Lens 1 (vacuum window)	>70% Transmission	>22% Transmission
MgF_2 Lens 2 (1550A only)	>70% Transmission	N/A
Filter	>10% Transmission	>10% Transmission
Mirror 3	>65% Reflectivity	>65% Reflectivity
Mirror 4	>65% Reflectivity	>65% Reflectivity
Phosphor Conversion Efficiency	>60%	>60%
Camera Collection Efficiency	>0.0011	0.0011
Total Efficiency	3×10^{-6}	4×10^{-7}

could have signal levels that exceed the minimum detection level for the CID camera by 1000× at 155 nm and 2× at 121.6 nm.

All of the optical housings are made from 304 or 316L stainless steel to resist the magnetically-induced eddy current forces and vessel disruption forces from the tokamak. No optical element adjustment mechanisms were provided due the space constraints and vacuum enclosures. Therefore, machining tolerances on the element mounting locations are kept to $\pm$ 50 µm to achieve sufficient image quality. From previous experience using a CIDTEC camera on the visible tangential TV, it was determined that the relay optics placed the image plane sufficiently far from the tokamak that the camera was not affected by magnetic field gradients. This eliminates the need to relay the phosphor image farther from the tokamak with a fiberroptic imageguide (as was done in the visible camera system) and avoids the problem of neutron induced browning in glass fiber imageguides.

A remotely actuated shutter system protects the sensitive optics during glow discharge cleaning and provides a heat shield during vessel baking (see Fig. 3).

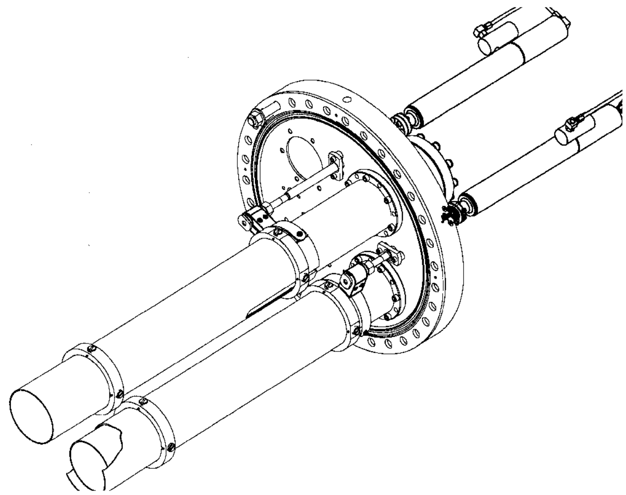

Fig. 3. A shutter system consisting of a radial tube which slides over the optical housing provides protection from plasma debris and the high vessel baking temperature.

The shutter consists of a movable radial concentric tube surrounding the in-vessel front mirror housing. The shutter tube is driven along the optic housing by a linear motion vacuum feedthrough. Radial bushings made of Vespel SP-1 center the shutter tube around the optical housing and provide a smooth bearing surface during actuation.

Bench alignment verification was performed using a HeNe laser that illuminated nine positions located around the object plane. A separte BK7 lens was inserted after the vacuum window to place the focus for the HeNe light (632.8 nm) at the same location as the 155 nm and 121.6 nm image positions. The CID camera then viewed this image plane to confirm that a clear field of view was achieved. We also measured a minimum resolution of 1 cm in the center of the field of view, which compares well with the predicted value of 1.2 cm.

III. FIRST IMAGE RESULTS

The diagnostic was commissioned on the DIII–D tokamak in several steps including imaging of visible emission, imaging of total VUV emission and finally imaging of the 155 nm CIV line emission. For the first series of tests the final MgF_2 lens was replaced by the BK7 visible imaging lens and both the 155 nm interference filter and phosphor were removed. Images of total visible emission from the DIII–D divertor were obtained. The system with the BK7 lens has optimal focus near the 656.1 nm D_α emission line from the divertor plasma. The images showed maximum intensity near the divertor tiles consistent with independent images of D_α from the visible camera system [Fig. 4(a)]. In addition, the images showed very good focus (1 cm gaps between the graphite tiles in the vessel were discernable) consistent with the laboratory tests done prior to installation. This verified that the mirrors and other optical components had survived a high temperature bake of the tokamak.

For the second series of tests, the BK7 lens was removed and the final MgF_2 lens was installed. The phosphor was also installed and the secondary vacuum was continuously pumped down to approximately 3 mTorr during the day of tokamak operations. Images of the phosphor response to the total VUV emission (wavelengths in the range 110–300 nm) were obtained. The lower wavelength limit was set by the MgF_2 cutoff wavelength; the higher limit is the wavelength at which the phosphor efficiency is down to approximately 1% of its peak value. The images with the maximum intensity [Fig. 4(b)] were obtained in moderate power (5 MW) plasma discharges with detachment induced by heavy deuterium gas puffing. Independent observations of CIII (456 nm) emission with the visible camera system confirmed the expectations

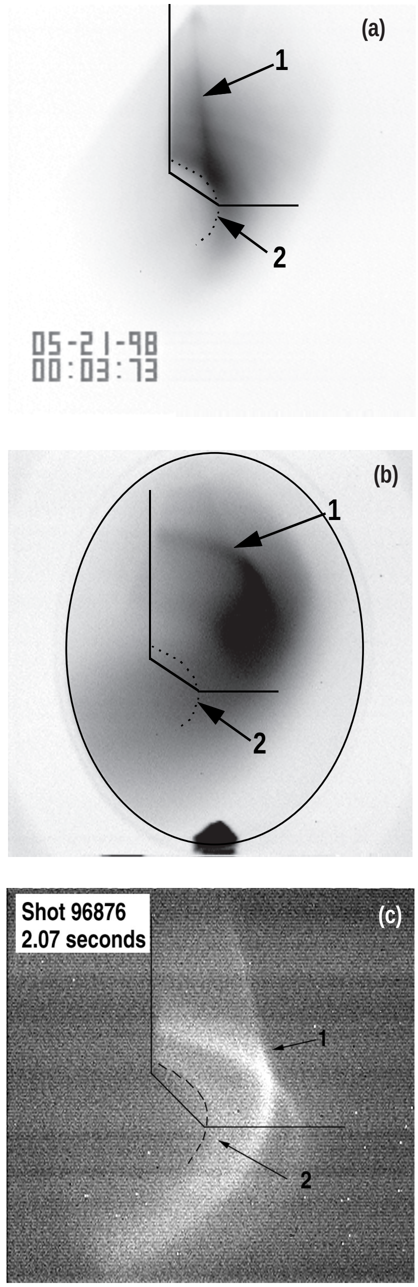

Fig. 4. First image data from a series of initial tests. The intersection of the tangency plane with the DIII–D inner wall, the 45 degree slanted tiles and the divertor floor are shown. In (b) and (c) the outline of the phosphor active area is also shown. In each case the arrow (1) shows the radiation in the vicinity of the X–point and the dashed arc (2) shows the intersection of the 45 degree tile face with the floor tiles. In a) an image of total visible light, using the BK7 focussing lens with the filter and phosphor removed, showing emission dominated by D_α radiation peaked near the floor and extending along the separtrix vertically, b) an image of total VUV emission, using the MgF_2 focusing lens and the phosphor, showing peaked emission near the X–point dominated by CIV (155 nm) radiation, and in c) filtered CIV emission, using the 155 nm filter with 20% transmission, again showing emission near the X–point.

that the carbon power would be localized near the X–point in this detached operation. The VUV image shows a peak emission in a toroidal ring near the location of the X–point and de-focused emission in other regions of the divertor. This is consistent with the interpretation that the ring is the CIV (155 nm) emission, for which the system focus should be optimum, and the additional emission is from other VUV lines (Ly-α at 121.6 nm or other carbon lines at 117.5, 133.5 and 136.4 nm).

The final tests were done with the 155 nm interference filter installed. Once again the brightest images [Fig. 4(c)] were obtained in the detached discharges (8 MW injected power). Peak transmission of the filter is calibrated at 20%, and the toroidal ring intensity, interpreted to be the CIV emission, was reduced about a factor of 5 from the images without the filter. These data show that the diagnostic images 155 nm emission from the DIII–D divertor. However, the intensity of the images is significantly less than our estimates from the transmissivities and reflectivities of the system components. Investigation of this discrepancy is in progress and optimization of the system throughput will be done during an extended maintenance period of the DIII–D tokamak. The geometry matrix needed to allow 2D profiles in a poloidal plane to be reconstructed from the 3D raw images will also be computed during the maintenance period so that the diagnostic can be used for physics studies when the tokamak resumes operations.

III. CONCLUSIONS

A diagnostic system capable of imaging the 155 nm emission from CIV was developed, installed and tested on the DIII–D tokamak. The system is also capable of imaging the 121.6 nm Ly-α emission from the deuterium plasma although this capability was not tested during the commissioning of the hardware. The system has a tangential view of the entire divertor region and provides a 2 m depth of field which allows emission from a large toroidal extent within the tokamak to be imaged. Data is recorded to VCR tape by a standard video camera for offline digitization and analysis. The diagnostic can withstand the high temperature (350°C) baking of the DIII–D vacuum vessel, and operates in the high neutron flux and electromagnetic radiation environment of the tokamak.

Initial tests verified that 155 nm emission (CIV) was imaged onto the video camera. The images were obtained using an interference filter with FWHM ~ 22 nm. Simultaneous independent measurements with the divertor SPRED spectrograph showed strong radiation at 155 nm with very weak continuum within the bandpass of the filter. Calculations indicated that wavelengths outside the filter bandpass would not be in focus. The strongest emission was observed in a toroidally continuous ring near the location of the X–point during partially detached divertor (PDD) operation induced by deuterium puffing. Simultaneous measurements of CIII (465 nm) visible emission with a separate tangentially viewing camera confirmed that the CIII radiation was localized near the X–point during the PDD. Previous theoretical work has shown that CIII and CIV radiation in PDD plasmas should occur within a few cm of each other. Combining this spatial correlation between visible and VUV cameras and the spectral verification of a single dominant line within the filter bandpass confirmed that the camera image was 155 nm radiation.

REFERENCES

[a]Present address: General Atomics, P.O. Box 85608, San Diego, California, 92186-5608.

[1]M.E. Fenstermacher, *et al.*, Rev., Sci. Instrum., **68**, 974 (1997).

[2]M.E. Fenstermacher, *et al.*, Physics of Plasmas, **4**, 1761 (1997).

[3]R.D. Wood, *et al.,* Proc. of the 23rd European Conference in Controlled Fusion and Plasma Physics, **20C**, 763 (EPS, 1996).

[4]R.D. Wood, *et al.,* Bull. Am. Phys. Soc. **42**, 1844 (1977).

ACKNOWLEDGEMENTS

We wish to thank Jim Weller for design support, Jeff Olsen for technical support, Lynn Seppala for optical analysis support, and Steve Allen for program support. This work was supported by the U.S. Department of Energy under Contract Nos. DE-AC03-89ER51114 and W-7405-ENG-48 and Grant No. 97ER54451.